Competition of synchronization domains in arrays of chaotic homoclinic systems.

I. Leyva[1,3],* E. Allaria[1], S. Boccaletti[1], and F.T. Arecchi[1,2]

[1] *Istituto Nazionale di Ottica Applicata, Largo E. Fermi 6, 50125 Florence, Italy*
[2] *Departement of Physics, University Of Firenze, Italy and*
[3] *Universidad Rey Juan Carlos. c/Tulipan s/n. 28933 Mostoles Madrid, Spain*

(Dated: February 4, 2003)

We investigate the response of an open chain of bidirectionally coupled chaotic homoclinic systems to external periodic stimuli. When one end of the chain is driven by a periodic signal, the system propagates a phase synchronization state in a certain range of coupling strengths and external frequencies. When two simultaneous forcings are applied at different points of the array, a rich phenomenology of stable competitive states is observed, including temporal alternation and spatial coexistence synchronization domains.

Synchronization of chaos refers to a process wherein two (or many) chaotic systems adjust a given property of their motion to a common behavior [1]. The emergence of synchronized features has been investigated in nature [2], in controlled laboratory experiments [3, 4], and the interest has moved toward the characterization of synchronization phenomena in spatially extended systems, such as large populations of coupled chaotic units and neural networks [5], globally or locally map lattices [6] and continuous space extended systems [7].

In this Letter, we consider a one dimensional chain of sites, each one undergoing a local homoclinic chaotic dynamics, interacting via a bidirectional nearest neighbor coupling. Homoclinic chaos consists of a train of nearly identical spikes separated by erratic inter-spikes intervals (ISI). In phase space, this motion corresponds to the passage through a saddle focus, where stable manifolds collapse and an unstable manifold emerges, with the expansion rate larger than the contraction one [8]. The saddle region displays a large susceptibility to an external stimulus, therefore such a chaotic system gets easily synchronized to a weak forcing signal.

The ability of such systems to synchronize to an external forcing was demonstrated in previous works [4], finding that it may constitute a reliable communication channel [9] robust against noise [10]. Furthermore, homoclinic chaos can be self-synchronized by feeding back a finite train of its own spikes, via either a delayed feedback [11] or a low frequency filter [12]; in this latter case obtaining a bursting behavior reminiscent of the dynamic of neurons in Central Pattern Generators [13].

However, when passing from a single system to an array, a relevant problem emerges related to the ability of the array to respond to external periodic perturbations localized at one end site, yielding synchronized patterns. The issue we are addressing is relevant for biological or artificial communication networks.

For convenience, we refer to a chain of dynamical units, each one represented by a 6-variable system modeling homoclinic chaos in a single mode CO_2 laser with feedback

[14]. The extension of the model to an array is:

$$
\begin{aligned}
\dot{x}_1^i &= k_0 x_1^i (x_2^i - 1 - k_1 \sin^2 x_6^i), \\
\dot{x}_2^i &= -\gamma_1 x_2^i - 2k_0 x_1^i x_2^i + g x_3^i + x_4^i + p, \\
\dot{x}_3^i &= -\gamma_1 x_3^i + g x_2^i + x_5^i + p, \\
\dot{x}_4^i &= -\gamma_2 x_4^i + z x_2^i + g x_5^i + z p, \\
\dot{x}_5^i &= -\gamma_2 x_5^i + z x_3^i + g x_4^i + z p, \\
\dot{x}_6^i &= -\beta[x_6^i - b_0 + r(\frac{x_1^i}{1+\alpha x_1^i} + \epsilon(x_1^{i-1} + x_1^{i+1} - 2 < x_1^i >))]
\end{aligned}
\tag{1}
$$

Here the index i denotes the ith site position ($i = 1, .., N$), and dots denote temporal derivatives. For each site, x_1 represents the laser intensity, x_2 the population inversion between the two levels resonant with the radiation field, and x_6 the feedback voltage which controls the cavity losses. The auxiliary variables x_3, x_4 and x_5 account for molecular exchanges between the two resonant levels and the other rotational levels of the same vibrational band. We consider identical units; as for the parameters, their physical meaning has been already discussed [14]. Their values are: $k_0 = 28.5714$, $k_1 = 4.5556$, $\gamma_1 = 10.0643$, $\gamma_2 = 1.0643$, $g = 0.05$, $p_0 = 0.016$, $z = 10$, $\beta = 0.4286$, $\alpha = 32.8767$, $r = 160$, $b_0 = 0.1032$.

The coupling on each site is realized by adding to the x_6 equation a function of the intensity (x_1) of the neighboring oscillators. The term $< x_1^i >$ represents the average value of the x_1^i variable, calculated as a moving average over the whole evolution time. The coupling strength $\epsilon > 0$ is our control parameter. The system is integrated by means of a standard fourth-order Runge-Kutta method with open boundary conditions.

We first study the emergence of synchronization in the absence of external stimuli, as the coupling strength ϵ increases. Due to the coupling, a spike on one site induces the onset of a spike in the neighbor sites as discussed in Ref. [15].

In Fig. 1(a)-(b) we show the transition from unsynchronized to synchronized regimes by a space time representation of the array. A detection threshold isolates the spikes getting rid of the chaotic small inter-spike back-
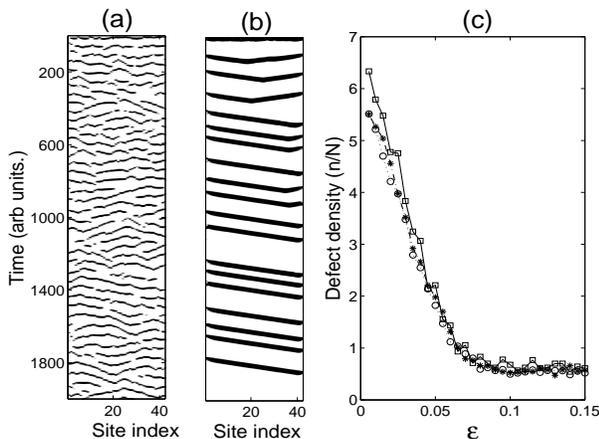
FIG. 1: Space-time representation of spikes positions for ϵ=0.05 (a) and ϵ=0.2 (b). (c) Average defect density vs. ϵ, for different chain lengths: N=10 ( ) , 40 ($\circ$), 80($*$).
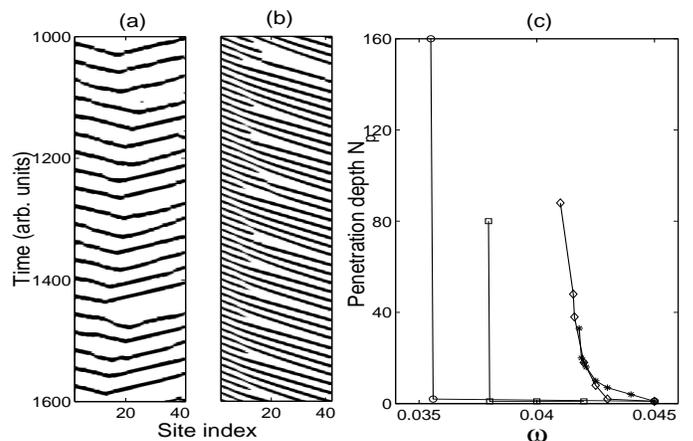

FIG. 2: Response of the N=40 chain with $\epsilon = 0.13$ and $\omega_o(\epsilon)$=0.02 to an external periodic forcing: (a) ω=0.015 , (b) ω=0.042. (c) Penetration depth vs. ω for different coupling strengths ϵ=: 0.12 ($*$), 0.15 ($\diamond$), 0.2 ( ), 0.25 ($\circ$).

ground, thus we plot only the spike positions as black dots. The transition to phase synchronization is anticipated by regimes where clusters of oscillators spike quasi-simultaneously [16]. Clusters are delimited by "phase slips" or defects, easily seen as holes in the space time fabric. More precisely, we introduce a phase measure $\phi^i(t)$ for a time interval t between two successive spikes of the same site, occurring at τ_{k-1}^i, τ_k^i, by linear interpolation [1]:

$$\phi^i(t) = 2\pi \frac{t - \tau_{k-1}^i}{\tau_k^i - \tau_{k-1}^i}. \qquad (2)$$

A defect appears as a 2π "phase slip" in the difference between the phases of two adjacent sites. Notice that this mutual referencing is the natural extension of measuring the regularity of a sequence against an external clock, whenever there is no external clock, but the time evolution of a site compares with the nearest neighbor sites. Hence "phase synchronization" denotes a connected line from left to right, not broken by defects. This definition of phase synchronization does not imply equal time occurrence, thus the unbroken lines are not isochronous as can be seen in Fig. 1 (b). The cluster size increases with ϵ extending eventually to the whole system (Fig. 1(b)). The route to phase synchronization can be characterized by the defect density, that is, the number of defects per site. In Fig. 1(c) we plot the average defect density as function of ϵ, calculated for a long evolution time ($T = 3 \times 10^5$). Full phase synchronization is reached when the defect density falls below one defect per site. The defect statistics has been studied for several chain lengths; we find that above N=30 there are no appreciable size-dependent effects. Once phase synchronization is established, a further increasing of ϵ reduces the natural frequency of the system $\omega_o(\epsilon) = \frac{2\pi}{<ISI>(\epsilon)}$. We will show

that this slowing down affects the capability of the array to synchronize to an external signal.

For this purpose, we explore the response of the system to an external periodic stimulus applied to the first site of the chain. Precisely, we periodically modulate the parameter b_o at the site $i = 1$ as $b_o^1 = b_o(t) = b_o(1 + A\sin(\omega t))$. From previous work, we know that this driving can induce a phase synchronization on a single oscillator [4]; here we explore the ability of the system to transmit the periodic signal through the chain.

The modulation amplitude A does not affect the results, provided that it is sufficient to synchronize the $i = 1$ site. Therefore, we do not loose generality by fixing a constant value $A = 0.3$.

We will consider that the signal has been successfully transmitted through the system when after a finite time the last element of the chain spikes with the same period of the external forcing, without defects. In Fig. 2 (a)-(b) we give examples of partial signal transmission. If ω is too small (Fig. 2 (a)) or too large (Fig. 2 (b)) with respect to the natural frequency of the system ($\omega_o(\epsilon)$=0.02 in the figure), then only partial transmission is achieved.

We explore the (ϵ, ω) range over which transmission propagates over the whole chain. In the low frequency limit, we find that $\omega < \omega_o(\epsilon)$ is not able to globally synchronize the chain. Independently of N, as ω_o is larger than ω, the last sites tend to spike spontaneously between two consecutive periods of the external driver before the synchronization propagates to them, and therefore synchronization is lost (Fig. 2 (a)).

When $\omega > 2\omega_o(\epsilon)$, the first N_p sites synchronize with the driving frequency, but beyond N_p a line of defects restores the natural oscillation regime (Fig. 2 (b)). This "penetration depth" N_p for synchronization is invariant
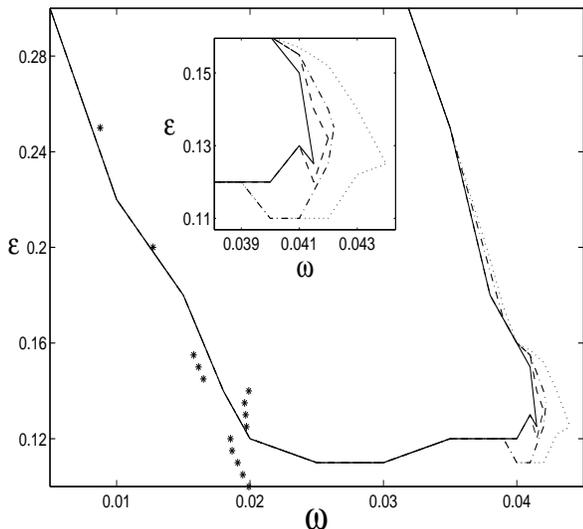
FIG. 3: Curves delimiting the (ϵ, ω) range for synchronized transmission in the arrays with lengths: N=10 (dotted lines), N=20 (dotted-dashed lines), N=40 (dashed lines) and N=80 (solid lines). The black stars indicate the average spiking frequency $\omega_o(\epsilon)$ of a site of the array in the absence of external perturbation. Inset: zoom of the area where the two external frequencies are selected for studying the spatial competition between synchronization domains.
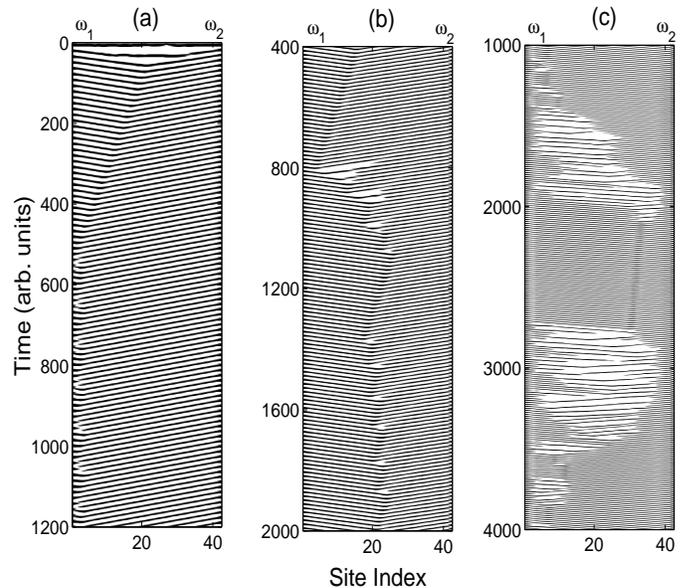

FIG. 4: Competition between spatial synchronization regimes induced by external forcing: (a) $\omega_1 = 0.02, \omega_2 = 0.021, \epsilon = 0.13$, (b) $\omega_1 = 0.038, \omega_2 = 0.042, \epsilon = 0.12$, (c) $\omega_1 = 0.04, \omega_2 = 0.0405, \epsilon = 0.11$

as we change the whole array length. In Fig. 2 (c) we plot the penetration depth vs. the forcing frequency for different values of ϵ. If for a point (ϵ, ω) the penetration depth is N_p, then one would observe complete synchronization only for sizes $N < N_p$, while incomplete synchronization would unavoidably take place for $N > N_p$. As a result, for a given N, only a limited range of external frequencies can be transmitted over the whole chain.

In Fig. 3 we plot the boundaries of the transmission band as a function of ϵ and ω, for several chain lengths. The region inside the curves contains all the (ϵ, ω) points for which global transmission is allowed. It can be seen that for each ϵ, the transmission band extends from ω_o (black stars) to approximately $2\omega_o$. Notice that the system starts to transmit for coupling strengths above the ones leading to intrinsic synchronization (approximately $\epsilon > 0.11$). For weaker couplings, the presence of defects breaks the continuity, while for $\epsilon > 0.35$ the homoclinic dynamics is destroyed. The left boundary of the transmission range refers to perfect transmission of the ω period up to the end of the chain. If one is only interested in the transmission of the average frequency, this boundary is slightly smeared out.

Now we have sufficient background to address the main question of how two different frequencies applied at the far ends of the chain compete in generating two separate spatial patterns of synchronization. The temporal competition between different synchronization states was re-

cently investigated theoretically [17] and experimentally [18] in the context of a single chaotic system forced by two external frequencies, finding competitive behaviors as alternations of synchronism to several frequencies $(\omega_1, \omega_2$ or a combination of the two). Here we go further addressing the problem of spatial competition between synchronization regions, which is preliminary to controlling the dynamics of an extended system as well as to studying the response of neural assemblies to competing external perturbations.

To answer this question, we apply to the first $(i = 1)$ and last $(i = N)$ site two periodic perturbations with frequencies ω_1 and ω_2, respectively. For simplicity, we will take always $\omega_o < \omega_1 < \omega_2$, so that $N_p(\omega_1) > N_p(\omega_2)$ (see Fig. 2 (c)).

The emerging competition scenario can be described with reference to Fig. 4. For $N_p(\omega_1), N_p(\omega_2) > N$, both frequencies synchronize over the whole chain. However, after a suitable transient time, the whole system synchronizes to the larger frequency ω_2, with the only exception of the site $i = 1$ (Fig. 4 (a)). This kind of "winner-takes-all" behavior is the consequence of the extended character of the system, and is at variance with the single oscillator behavior for both forcing frequencies inside the Arnold tongue. In fact, in Ref. [17] the entrainment takes place at the frequency closer to the natural frequency ω_o.

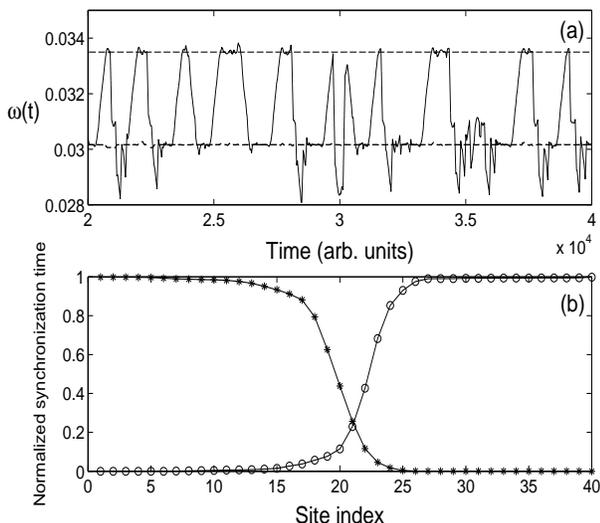For $N_p(\omega_1) > N, N_p(\omega_2) < N$, only the smaller frequency synchronizes over the whole chain, while the

FIG. 5: (a) Time evolution of $\omega(t)$ for i=1 and i=40 (dashed lines) and for the site i=22 (solid line) located on the domain boundary for the case of Fig. 4 (b). (b) Normalized locking time at the frequencies ω_1 ($*$) and ω_2 ($\circ$) vs. site index for the whole chain.

larger frequency is limited to the $N_p(\omega_2)$ sites closest to $i = N$. In this situation, we find that permanent synchronization domains for ω_1 and ω_2 are established, with an irregular domain wall (Fig 4 (b)). If we increase N, the ω_2 domain is always confined to the last $N_p(\omega_2)$ sites, independently of the total length of the chain as well as of the value of ω_1. The domains are stable, as checked with a very long integration time ($T > 3 \times 10^7$). For the case of Fig 4 (b), we plot the instantaneous frequency [1] for $i = 1, i = 40$ and $i = 22$ (Fig. 5 (a)). It can be observed that the site $i = 22$ located on the domain boundary locks alternatively to ω_1 and ω_2. The locking periods are interrupted by defects. In Fig 5 (b), we plot the normalized locking time of all sites to ω_1 and ω_2, respectively. The transition is smooth spacewise and the boundary layer has a width of approximately 6 sites, independently of the chain length.

Finally, for $N_p(\omega_1)$, $N_p(\omega_2) < N$, neither of the two frequencies stabilizes a synchronized pattern over the whole chain. In this case, we observe alternation between synchronization patterns with frequencies ω_1 and ω_2, with intervals of asynchrony filled with defects, as shown in Fig 4 (c). The duration of the synchrony and asynchrony intervals is irregular. This competitive behavior persists in time. As a consequence, the competition between the two frequencies has here a cooperative effect, insofar as it enhances the ability of each single entrainment process to reach global synchronization over finite time slots.

In summary, we have studied the response of a chain of nearest neighbor coupled homoclinic oscillators to periodic stimuli. The array can propagate a synchronization state in a range of couplings and external frequencies (ϵ, ω). When two simultaneous forcings are applied at different points of the array, a rich phenomenology of stable competitive states is observed. The features and stability of these states depend on the intrinsic dynamics of the system independently of the chain size.

---

* Electronic address: ileyva@ino.it

[1] For a review of the subject see A. Pikovsky, M. Rosenblum and J. Kurths, *Synchronization: A Universal Concept in Nonlinear Sciences*, (Cambridge University Press, 2001); S. Boccaletti, J. Kurths, G. Osipov, D. Valladares and C. Zhou, Phys. Rep. **366**, 1, (2002).

[2] C. Schafer, M. G. Rosemblum, J. Kurths and H. H. Abel , Nature **392**, 239 (1998); G.D. Van Wiggeren and R. Roy, Science **279**, 1198 (1998); B. Blasius, A. Huppert and L. Stone, Nature, **399**, 354 (1999).

[3] C.M. Ticos, E. Rosa Jr., W. B. Pando, J. A. Walkenstein and M. Monti, Phys. Rev. Lett. **85**, 2929 (2000); D. Maza, A. Vallone, H. Mancini and S. Boccaletti, Phys. Rev. Lett. **85**, 5567 (2000).

[4] E. Allaria, F. T. Arecchi, A. Di Garbo and R. Meucci, Phys. Rev. Lett. **86**, 791 (2001); S. Boccaletti, E. Allaria R. Meucci and F. T. Arecchi. Phys. Rev. Lett. **89**, 194101 (2002) .

[5] S. H. Strogatz, S.E. Mirollo and P.C. Matthews, Phys. Rev. Lett. **68**, 2730 (1992); V. N. Belykh, I. Belykh and M. Hasler, Phys. Rev. E **63**, 036216 (2001).

[6] V. N. Belykh and E. Mosekilde, Phys. Rev. **E54**, 3196 (1996); A. Pikovsky, O. Popovich and Yu. Maistrenko, Phys. Rev. Lett. **87**, 044102 (2001).

[7] S. Boccaletti, J. Bragard, F. T. Arecchi and H. Mancini, Phys. Rev. Lett. **83**, 536 (1999); L. Junge and U. Parlitz, Phys. Rev. **E 62**, 438, (2000).

[8] L. P. Sil'nikov, Sov. Math. Dokl. **6**, 163 (1965).

[9] I.P. Mariño, E. Allaria, R. Meucci, S. Boccaletti and F.T. Arecchi. Chaos (in press, March 2003).

[10] C.S. Zhou, J. Kurths, E. Alaria, S. Boccaletti, R. Meucci and F.T. Arecchi, Phys. Rev. E **67**, 15205 (2003).

[11] F.T. Arecchi, R. Meucci, E. Allaria, A. Di Garbo and L.S. T Simring, Phys. Rev. E **67**, 46237 (2002).

[12] R. Meucci, A. Di Garbo, E. Allaria and F. T. Arecchi, Phys. Rev. Lett. **88**, 144101 (2002).

[13] R. C. Elson, A. I. Selverston, R. Huerta, N. F. Rulkov, M. I. Rabinovich, and H.D. I. Abarbanel, Phys. Rev. Lett **81**, 5692 (1998).

[14] A.N. Pisarchik, R. Meucci and F.T. Arecchi, Eur. Phys. J. D **13**, 385 (2001).

[15] I. Leyva, E. Allaria, S. Boccaletti and F. T. Arecchi, submitted to Phys. Rev. E (e-print: nlin.PS/0210042).

[16] Z. Zheng, G. Huand and B. Hu, Phys. Rev. Lett. **81**, 5318 (1998)

[17] R. Breham and E. Ott, Phys. Rev E **65** 056219 (2002).

[18] R. Allister, R. Meucci, D. DeShazer and R. Roy, Phys. Rev E **65** 015202(R) (2003).